Aerosol Science and Technology

ISSN: 0278-6826 (Print) 1521-7388 (Online) Journal homepage: http://www.tandfonline.com/loi/uast20

A High Volume Apparatus for the Condensational Growth of Ultrafine Particles for Inhalation Toxicological Studies

Philip Demokritou , Tarun Gupta & Petros Koutrakis

To cite this article: Philip Demokritou , Tarun Gupta & Petros Koutrakis (2002) A High Volume Apparatus for the Condensational Growth of Ultrafine Particles for Inhalation Toxicological Studies, Aerosol Science and Technology, 36:11, 1061-1072, DOI: 10.1080/02786820290092230

To link to this article: http://dx.doi.org/10.1080/02786820290092230

Published online: 30 Nov 2010.

Submit your article to this journal

Article views: 153

View related articles

Citing articles: 15 View citing articles

Full Terms & Conditions of access and use can be found at
http://www.tandfonline.com/action/journalInformation?journalCode=uast20

Download by: [University of North Texas] **Date:** 06 January 2017, At: 21:59

Aerosol Science and Technology 36: 1061–1072 (2002)
© 2002 American Association for Aerosol Research
Published by Taylor and Francis
0278-6826/02/$12.00 + .00
DOI: 10.1080/0278682029009223 0

A High Volume Apparatus for the Condensational Growth of Ultrafine Particles for Inhalation Toxicological Studies

Philip Demokritou, Tarun Gupta, and Petros Koutrakis
Environmental Science and Engineering Program, School of Public Health, Harvard University, Boston, Massachusetts

A high volume (2500 LPM) system for the condensational growth of ultrafine particles was developed and evaluated using indoor air as a test aerosol. The main features of this system are the following: (a) ultrafine particles grow condensationally to supermicron sizes using high purity deionized water as a condensing medium; (b) the supersaturation ratio is adjustable and can be precisely controlled; (c) the system can operate for a wide range of ambient air temperature and relative humidity conditions; and (d) a thermal dryer is used to return the condensationally grown particles back to their original size. Restoring the original ambient size distribution and preserving the composition of the ambient ultrafine particles is very important for inhalation studies.

The system is fully automated and has computerized feedback controls. In addition, saturation of the aerosol with water vapor occurs at close to ambient temperatures to minimize particle losses of volatile components. Saturation of sample air is obtained using a direct steam-injecting, fully modulating electric humidifier. The sample air after saturation is drawn through the supersaturator, which is a refrigerant-to-air heat exchanger and is cooled down to obtain the desirable supersaturation ratio. Supersaturation ratios can be precisely adjusted, with the optimum operational level found to be in the range of 2 to 3. The performance of the system was evaluated as a function of critical operation parameters, including the supersaturation ratio as well as the saturation and supersaturation temperatures. A series of virtual and conventional impactors was used to characterize the condensational growth of ultrafine particles. This new high volume apparatus was shown to grow ambient ultrafine particles to supermicron sizes with a particle size growth of approximately 1.8 μm. Particle losses in the system were found to be minimal (about 10%). The thermal dryer was used successfully to restore the grown particles back to their original size distribution. Particle concentration, aerosol temperature, and residence time (aerosol flow) are key parameters shown to affect the performance of the thermal dryer.

Received 16 November 2001; accepted 19 March 2002.
This laboratory performance evaluation of the high volume condensational growth system was supported by U.S. EPA STAR grant R825 270-01-0 and the EPA/Harvard Particle Health Effects Center (EPA grant R827353-01-0).
Address correspondence to Philip Demokritou, Ph.D., Environmental Science and Engineering Program, Department of Environmental Health, Harvard School of Public Health, 401 Park Drive, PO Box 15677, Landmark Center West, Room 421, Boston, MA 02215. E-mail: pdemokri@hsph.harvard.edu

INTRODUCTION

Ultrafine particles (aerodynamic diameter, $d \leq 0.1$ μm) are formed through gas-to-particle conversion mechanisms. Ultrafine particles are associated both with natural and anthropogenic sources (Kavouraset al. 1998; Whitby and Svendrup 1980; Kotzick and Niessner 1999). Due to phase transformation processes, which become more enhanced as particle size decreases, ultrafine particle sizes change continuously (Seinfeld 1991).

Epidemiological studies have reported significant associations between $PM_{2.5}$ and PM_{10} and increased mortality and morbidity (Schwartz and Dockery 1992; Dockery et al. 1993; Dockery and Pope 1994; Gamble 1998; Pope et al. 1999; Peters et al. 2000). Inhaled ultrafine particles deposit almost exclusively in the respiratory tract by diffusional mechanisms (ICRP 1994). The pulmonary toxicity of ultrafine particles has been demonstrated in several controlled laboratory exposure studies. Inhalation of fumes, consisting mainly of ultrafine particles, lead to the well-known effects of metal or polymer fume fever (Drinker et al. 1927; Gordon et al. 1992). Oberdorster et al. (1994) showed that inhaled ultrafine particles could cause great impairment to the alveolar macrophage clearance function. It has been speculated that the increased pulmonary toxicity of these particles may be due to their high surface area to volume ratio and their ability to penetrate the alveolar epithelium. Notwithstanding these findings, the health effects of ambient ultrafine particles have not yet been fully investigated. This is largely due to the lack of particle generation methods that can be used to expose human and animal models to "real world" ambient air ultrafine particles.

The development of high volume slit nozzle virtual impactors made it possible to expose humans and animals to ambient fine

particles (2.5 μm $\leq$ size $\leq$ 0.15 μm) concentrated by a factor of about 30. In particular, the fine particle concentrator developed at the Harvard School of Public Health (Sioutaset al. 1995) has been successfully used during the last 5 years for human and animal inhalation studies (Godleski et al. 1996; Clarket al. 2000). Also, a two stage, low particle loss, high volume coarse particle concentrator has recently been developed using a slit nozzle technology that is capable of concentrating ambient coarse particles up to 60 times (Demokritou et al. 2001). In the past, hypersonic virtual impactors operating at very low pressures ($\sim$500 Pa or less) have been developed and used to collect ultrafine particles (de la Mora et al. 1990; Hering and Stolzenburgh 1995; Olawoyin et al. 1995). However, use of hypersonic virtual impactors to concentrate ultrafine particles has the following limitations: (a) it is not feasible to conduct animal or human exposures at very low pressures; (b) losses of ultrafine semivolatile constituents can be significant at such low pressure conditions; and (c) high sampling flow rates (1000 L/min or higher) can only be achieved by operating thousands of such impactors in parallel.

A new approach was recently developed to inertially separate and concentrate ultrafine particles from the majority of the surrounding air without subjecting them to excessively low pressures (Sioutas and Koutrakis 1996; Sioutas et al. 1999; Kidwell and Ondov 2001). This method uses condensational growth to enlarge particles above 1 μm. Subsequently, the grown particles are concentrated using a round nozzle virtual impactor. However, these systems are restricted to a limited aerosol input flow (about 100 LPM) and a limited output flow. To achieve the necessary flow, a large number of systems would have to be operated in parallel. In addition, these systems operate at low and uncontrolled supersaturation ratios that depend on the temperature and humidity of the ambient air.

Condensational growth of particles in the atmosphere is a well-known phenomenon and has been extensively investigated since the pioneering studies of Aitken (1888). The adiabatic expansion of air masses results in supersaturation conditions that lead to the activation and growth of nanoparticles to supermicron sizes. This leads to cloud formation, where ultrafine particles act as condensation nuclei to form water droplets. Condensational growth of ultrafine particles has been used over the years by scientists for their detection. The condensation nuclei counter (CNC) is the most widely used instrument for submicron particle measurements. According to this method, particles grow using a supersaturated vapor to a sufficiently large size for easy detection and quantification by optical methods (Bricard et al. 1976; Sinclair and Hoops 1975; Agarwal and Sem 1980). The aerosol is first exposed to the vapor of a working fluid (i.e., butanol, alcohol, or water) in a saturation chamber. Subsequently, vapor condensation onto particles is induced by either adiabatic expansion or cooling in the condensing chamber. The formed droplets are then detected using light scattering or attenuation measurement techniques (Ahn and Liu 1990). These instruments traditionally have a relatively low sampling flow rate ranging from 2.8 to 28 LPM. Although CNCs are excellent tools for the quantification of ultrafine particles, their relatively low flow rates as well as the use of toxic working fluids (i.e., butanol) prohibits their use in inhalation and toxicological studies.

In this paper, we present the development and laboratory performance evaluation of a high volume (2500 LPM) system for the condensational growth of ultrafine particles. The main features of this method are the following: (a) particle condensational growth is achieved at near ambient aerosol temperature; (b) supersaturation ratios are adjustable to as high as 6 (normal operation level is between 2 and 3); (c) the system can operate for a wide range of ambient air temperature and relative humidity conditions; and (d) particle size distribution restoration is obtained using a thermal drying method. This thermal drying method overcomes the limitations of diffusion drying techniques, which were previously used for low flow ultrafine concentrator prototypes.

CONDENSATIONAL GROWTH OF PARTICLES

Air supersaturation can be achieved either by cooling or adiabatic expansion. Under such conditions, the condensing vapor (in our system, deionized water is used) condenses onto the particle surface to form droplets of a bigger size. The supersaturation ratio (S_R) is an important parameter affecting the particle size changes. S_R is defined as the ratio of the water vapor partial pressure, at temperature T(K), to the water saturation vapor pressure at the same temperature (Hinds 1999):

$$S_R = \frac{p}{p_s}, \qquad [1]$$

where p is the water vapor pressure (Pa) and p_s is the saturation pressure of water vapor (Pa).

The water vapor saturation pressure (p_s) over a flat water surface, for a temperature range of 273 to 330 K, can be calculated using the following empirical correlation (Hinds 1999):

$$p_s = exp\left(16.7 - \frac{4060}{T - 37}\right)(\text{kPa}). \qquad [2]$$

For pure liquids, the relationship between the saturation ratio required for equilibrium (no growth or evaporation), called the Kelvin ratio, K_R, and the droplet size (d^*) is given by the Kelvin equation (Hinds 1999):

$$S_R = K_R = \frac{p_d}{p_s} = exp\left[\frac{4\gamma M}{\rho_p R T d^*}\right], \qquad [3]$$

where K_R is the Kelvin ratio, p_d is the water vapor pressure at the particle surface, γ, M, and ρ_p are the surface tension, molecular weight, and density of water, and d^* is the Kelvin diameter.

For pure liquids at a given supersaturation ratio, particles larger than the Kelvin diameter will grow, while those smaller than d^* will be too small to initiate vapor condensation. However, in the presence of condensation nuclei or ions, particle growth can occur at supersaturation ratios of only a few percent and

for water-soluble nuclei at even unsaturated conditions (Hinds 1999). Furthermore, it was shown in theoretical and experimental studies that certain types of particles, such as soot particles, need a much higher supersaturation ratio than the theoretical to initiate growth (Kotzick et al. 1997).

The droplet rate of growth by condensation for $d_p < \lambda_w$ can be calculated by the following equation (Hinds 1999):

$$\frac{d}{dt}(d_p) = \frac{2\alpha_c}{\rho_p\sqrt{\frac{2\pi RT}{M}}}(p - p_d). \quad [4]$$

For $d_{\hat{p}} > \lambda_w$ the droplet rate of growth can be calculated by the following equation (Zhang and Liu 1990):

$$d_p\frac{d}{dt}(d_p) = \frac{4D_wM}{R_{\rho_p}}\left(\frac{p}{T} - \frac{p_d}{T_d}\right)f(Kn_w), \quad [5]$$

where

$$f(Kn_w) = \frac{1 + Kn_w}{1 + 1.71Kn_w + 1.333Kn_w^2} \quad \text{(Fuchs and Sutugin 1970)}, \quad [6]$$

$$Kn_w = \frac{2\lambda_w}{d_p}, \quad [7]$$

where $\lambda_w = 0.0673$ μm is the mean free path of the water vapor molecules in air (at 23°C; Ferron and Soderholm (1990)), $\lambda_a = 0.066$ μm is the mean free path for air molecules (at 1 atm, 20°C; Hinds (1999)), Kn_w is the Knudsen number based on the water vapor mean free path in air (unitless), Kn_a is the Knudsen number based on the mean free path of air molecules (unitless), α_c is the condensation coefficient (0.04; Hinds (1999)), D_w is the diffusion coefficient of water vapor in air (m^2s^{-1}), T_d is the temperature at the surface of the droplet (K), T is the gas temperature away from the droplet (K), R is the ideal gas constant ($NmK^{-1}mol^{-1}$), L is the latent heat of condensing water vapor (Jkg^{-1}), and k_a is the heat conductivity of air ($Jm^{-1}s^{-1}K^{-1}$).

During condensation, droplet heating takes place due to the release of the latent heat of vaporization. An equilibrium droplet temperature is approached by balancing the heat gained due to latent heat with the heat lost by conduction to the cooler surrounding air. The temperature on the droplet surface, T_d, can be obtained from the numerical solution (using fourth-order Runge-Kutta method) of the following equation (Ahn and Liu 1990):

$$T_d = T + \frac{D_wML}{Rk_a}\left(\frac{p}{T} - \frac{p_d}{T_d}\right)\frac{f(Kn_w)}{f(Kn_a)}, \quad [8]$$

where

$$f(Kn_a) = \frac{1 + Kn_a}{1 + 1.71Kn_a + 1.333Kn_a^2} \quad \text{(Fuchs and Sutugin 1970)}, \quad [9]$$

$$Kn_a = \frac{2\lambda_a}{d_p}. \quad [10]$$

For $d_p > \lambda_w$, the value of T_d can be estimated for S_R ratios up to 5 and an ambient temperature range of 0 to 40°C, as follows (Hinds 1999):

$$T_d = T + \frac{(6.65 + 0.345T + 0.0031T^2)(S_R - 1)}{1 + (0.082 + 0.00782T)S_R}. \quad [11]$$

A condensational growth system consists of 2 main components: (i) the saturator where air saturation takes place, and (ii) the supersaturator or condenser where vapor condensation on particles occurs. Based on the aforementioned thermodynamic model, which describes the fundamental heat and mass transfer processes, for a given saturator temperature, T_s, and a condenser temperature, T_c, the theoretical supersaturation ratio can be calculated. Figure 1 shows the relationship between supersaturation ratio and condenser temperature for different saturation temperatures. For a given supersaturation ratio, the thermodynamic model can also be used to calculate the growth rate as a function of time. Figure 2 shows the growth of a 0.07 μm particle as a function of time at different supersaturation ratios. One can conclude that for higher supersaturation ratios, ultrafine particle sizes increase faster.

Furthermore, it is important to examine the vapor concentration and temperature profile inside the condenser tubes. The concentration of water vapor and the air temperature inside a condenser tube are functions of the distance from the tube entrance and are related to the transport phenomena in the tube (transfer of heat, mass, and momentum). As a result, the supersaturation ratio is also a function of the distance from the tube entrance. This was shown in numerical and experimental studies (Zhang and Liu 1990). These studies showed that the higher saturation ratios occur at the radial center of the tube, mainly due to condensation on the tube wall. Due to this radial gradient of the vapor concentration in the tube, not all particles of a given initial size are expected to grow to the same extent. In addition, since the condensation rate on the tube wall is itself a function of the tube length, there is a gradual decrease in total vapor concentration as the sample air passes through the condenser, which further complicates the pattern of particle growth. Moreover, since the growth rate also depends on initial particle size, a heterogeneous particle growth is expected within the condenser tube. Finally, the actual supersaturation ratio, at the different points of the system, may differ from the theoretically calculated using the average condenser entrance and exit conditions.

METHODS

Description of the System

The high volume system for the condensational growth of ultrafine particles is shown in Figure 3. The system consists of 3 major components: the preheater section, the saturator, and the condenser or supersaturator. The preheater is an electric coil installed in the duct and used to preheat the incoming air up to 20°C when the temperature of the incoming sample air is <20°C

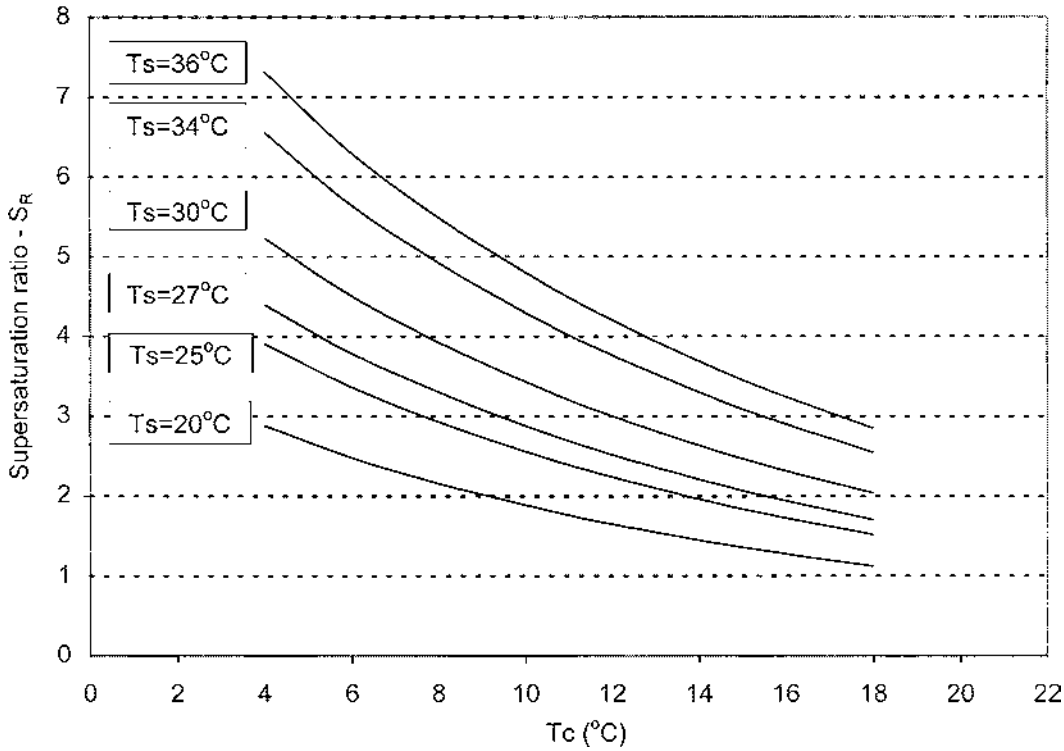

Figure 1. Supersaturation ratio as a function of condenser (*Tc*) and saturator (*Ts*) temperatures.

(winter conditions). Otherwise no preheating is provided. Preheating of air enhances the saturation process because it allows the incoming air to more efficiently absorb the steam injected into the saturator section. The saturator is a 1.5 m long, 12.5 cm diameter round duct. The steam injection tube is located inside the saturator, near the entrance. As the air passes by, steam is injected and mixed with the air. The flow inside the saturator is turbulent (Re > 2300) to enhance steam mixing. Steam is generated using a fully modulated, electric humidifier. To avoid formation of particles during the humidification process, high purity

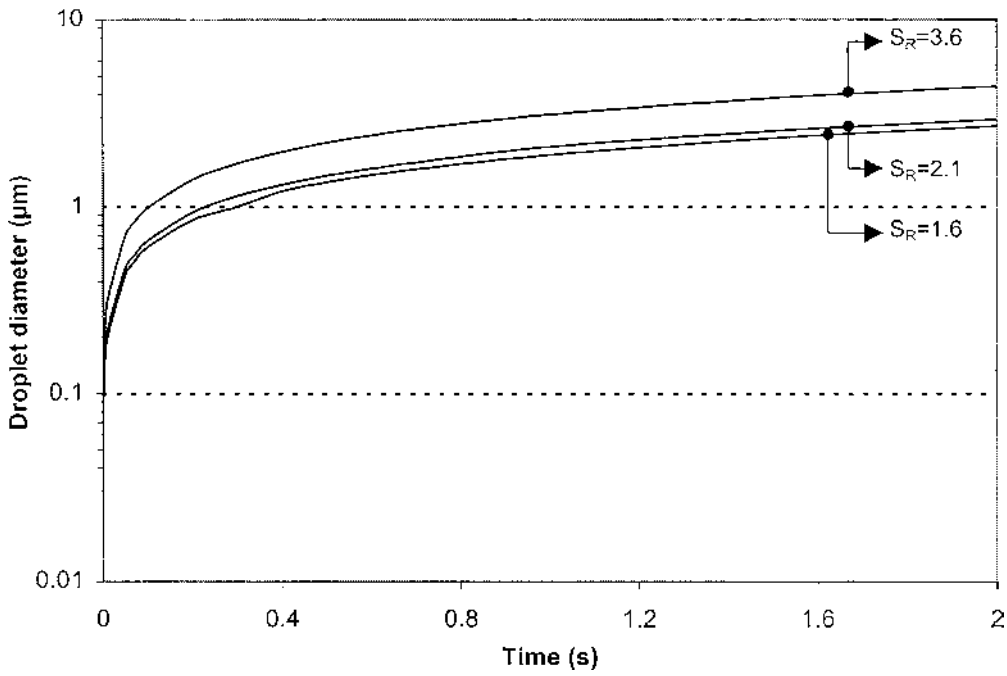

Figure 2. Condensational growth of a 0.07 μm particle as a function of time at different supersaturation ratios.

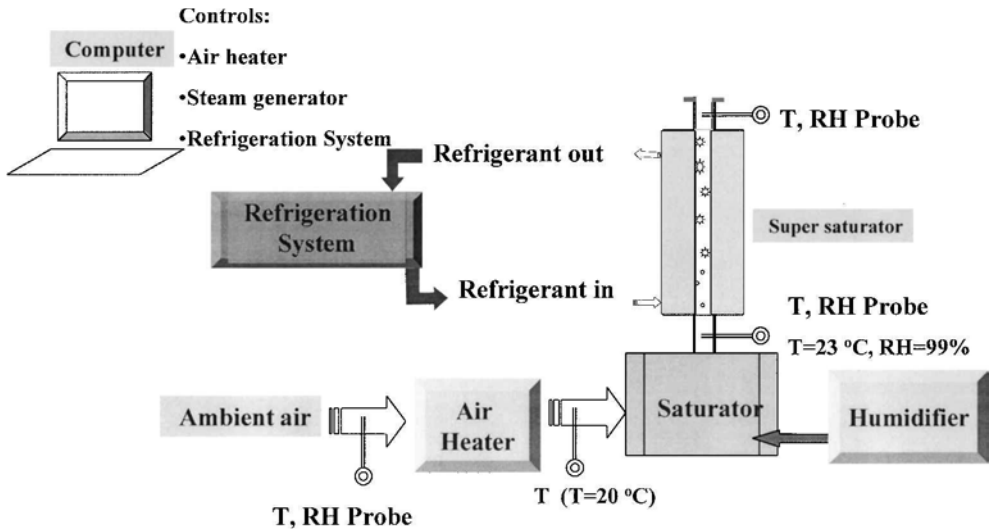

Figure 3. High volume condensational growth apparatus (HVCGA).

deionized water is used (Milli-Q water or equivalent: resistivity 18.2 megaohm; total organic compounds <10 ppb; particle-free <0.2 μm; bacteria <1 colony forming unit/mL). Tests showed no ultrafine particle generation from the humidification process.

The sample air exits the saturator at close to saturation conditions (relative humidity near 99%) and with a temperature increase of <2°C, minimizing losses of semivolatile components of ultrafine particles. Subsequently, sample air enters the condenser (supersaturator), where it cools down and achieves the target supersaturation ratio. The apparatus can produce controlled supersaturation ratios of up to 6. However, the normal supersaturation ratio of our system is approximately in the range of 2 to 3.

The condenser is a shell-and-tube type refrigerant-to-air heat exchanger, with the air flowing through the tubes and the refrigerant through the shell side. Airflow through each tube is laminar to minimize particle losses, with residence time of about 0.6 s. A direct expansion refrigeration system was built to provide the required medium (refrigerant) for the cooling. The refrigerant temperature inside the heat exchanger is adjustable. The refrigeration system is fully automated. A computerized system is used to monitor and control the operational parameters of the high volume condensational growth apparatus (HVCGA), including relative humidity; air temperatures; refrigerant temperatures; and airflow in every component of the system. A single pump, which operates at a flow rate of 2500 LPM, was used. Pressure drop through the system is only about 1.1 kPa, which is adequately low for inhalation toxicological chamber tests.

Experimental Setup

The experimental setup used to test the ultrafine particle growth system is schematically illustrated in Figure 4. A variety of particle sampling devices were employed to investigate the particle growth, including the (cascade) micro-orifice impactor (MOI) (Marple et al. 1991), the dichotomous sampler (Ding and Koutrakis 2000), the high volume virtual impactor (HVVI, MSP, MN), and the Harvard coarse particle concentrator (HCPC) (Demokritou et al. 2001); see Table 1. For flow values different from the nominal (original design) values, the 50% cutpoint (d_{50}) of the virtual impactors was calculated theoretically. For these calculations the value of $\sqrt{\mathrm{St}}$ (square root of Stokes number) was assumed to be 0.5. This was based on theoretical and experimental analyses of virtual impactors with a minor to total flow ratio of 0.1 (Marple and Chien 1980).

Both conventional and virtual inertial impactors were used to investigate particle growth. All virtual impactors operated at flow rates that were expected to yield cutpoints between 0.6 and 2.5 μm, considerably larger than the ultrafine mode ($d < 0.1$ μm). Room air was used as the test aerosol and was drawn through the high volume condensational growth apparatus at a flow of 2500 LPM. At the exit of the condenser, a fraction of the air sample was drawn through a virtual or conventional impactor. The particle number concentration was measured for 5 min intervals using a condensation particle counter (CPC 3010A, TSI Inc., St Paul, MN). Size distribution was also measured using a scanning mobility particle sizer (SMPS, TSI Inc., St. Paul, MN). Since room air was used as the test aerosol, its particle number concentration is virtually the same as the ultrafine particle number concentration. Therefore, CPC measures with a very good approximation the ultrafine particle number concentrations. Measurements were conducted at the minor flow of the virtual impactors and downstream of the impaction substrate of the conventional impactor. In addition, particle concentration and size distribution of the inlet air was measured. The concentration enrichment factor (CEF), defined as the ratio of the minor to incoming (ambient) number particle concentration, was calculated for the virtual impactor experiments. Also, the particle penetration efficiency, defined as the percentage of the ambient particles penetrating the conventional impactor, was calculated for the conventional impactor experiments. The effect

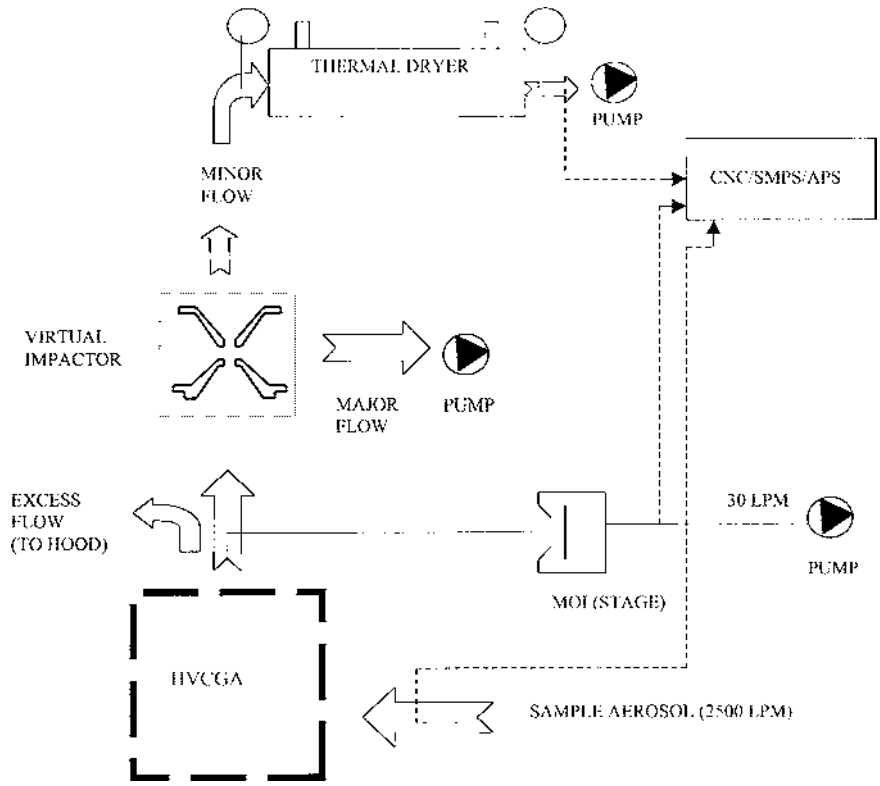

Figure 4. Experimental setup for the characterization of HVCGA.

of condenser temperature, saturation temperature, and supersaturation ratio on ultrafine particle growth were also investigated.

Restoring of the distorted ultrafine particle size distribution to its original one is of paramount importance for inhalation studies since particle dose depends on particle size. This can be achieved by evaporating the water from the formed droplets. In the past, diffusion dryers have been used to dry grown ultrafine particles (Kim et al. 2000). Shortcomings associated with the use of diffusion dryers include saturation of the desiccant in a short period of time and relatively low aerosol flow capability. To overcome these limitations, a thermal method was used to dry and consequently restore the ultrafine particles to their original size distribution. The thermal drying system consists of parallel electrically heated tubes (i.d., 5 cm, length: 1.5 m). Aerosol

Table 1
Main characteristics of impactors used in the study

Name	Type	Flow (LPM)	d_{50} (μm)	Reference
MOI	Conventional impactor			Marple et al. 1991
Stage #2		30	6.2	
Stage #3		30	3.2	
Stage #4		30	1.8	
Stage #5		30	1.0	
Dichotomous sampler	Virtual impactor	16.7	2.5	Ding and Koutrakis 2000
		35	1.7*	
		60	1.3*	
HVVI	Virtual impactor	150	1.0	HVVI, MSP, MN
		350	0.6*	
HCPC	Virtual impactor	2000	1.2	Demokritou et al. 2001

*d_{50} values at flow rates different from the nominal ones (original design) were theoretically calculated (assuming $\sqrt{\mathrm{St}} = 0.5$).

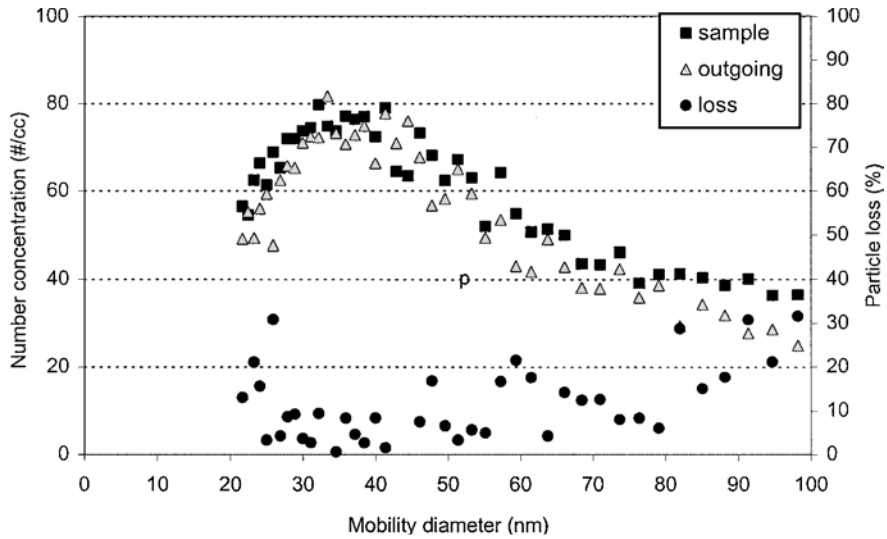

Figure 5. Particle losses as a function of mobility diameter for the HVCGA.

temperatures at both the entrance and exit of the dryer were monitored and controlled. The size distribution of particles at the exit of the thermal dryer was measured using an aerodynamic particle sizer (APS 3320, TSI, Inc., St. Paul, MN) and a SMPS (TSI Inc., St. Paul, MN). Aerosol flow through the dryer was also measured. Finally, the performance of the thermal dryer was investigated as a function of critical parameters, such as aerosol temperature, aerosol concentration, and residence time.

RESULTS AND DISCUSSION

A number of performance evaluation tests were conducted using indoor air as the test aerosol. The preheater was used to vary the saturation temperature, and thus the sampling air temperature. Saturator air temperature and relative humidity ranged between 25 and 34°C and 20 and 100%, respectively. The system is fully automated with computer feedback controls and it showed an excellent ability to maintain stable temperature and relative humidity settings in its various components for durations of several hours.

Ultrafine particle losses throughout the system were <10% and were independent of initial size. Therefore changes in particle size distribution due to internal losses during growth are expected to be negligible. Figure 5 illustrates the measured ultrafine particle losses as a function of the particle size.

MOI Experiments

Table 2 summarizes the results from the MOI tests. These findings suggest that particle growth depends on the

Table 2
MOI experimental results

	Saturator		Condenser					
d_{50} (μm)	T (°C)	RH (%)	T (°C)	RH (%)	Saturation ratio S_R	Ambient conc. (#/cm^3)	Downstream conc. (#/cm^3)	Penetration (%)
6.2	25	20	12	95	0.45	35000	28700	82
6.2	25	97	12	95	2.91	35000	31000	89
3.1	31	20	14	95	0.56	37000	26000	70
3.1	31	100	14	95	2.81	37000	17000	46
3.1	34	100	15	95	3.12	37000	12000	32
3.1	34	100	15	95	3.12	37000	10500	28
1.8	25	20	12	95	0.45	33000	22000	67
1.8	28	67	13	95	1.69	33000	24000	73
1.8	27	97	13	95	2.31	33000	9000	27
1.8	33	100	15	95	2.95	33000	4000	12
1.0	25	20	13	95	0.42	42000	27000	64
1.0	29	99	14	95	2.48	42000	18000	43
1.0	32	100	15	95	2.79	42000	10000	24
1.0	34	100	16	95	2.93	42000	4000	9

Table 3
Performance of concentrators under various operation conditions

Virtual impactor	d_{50} (μm)	$^a r$ (%)	Total flow (LPM)	Ambient air T (°C)	Saturator T (°C)	Saturator RH (%)	Condenser T (°C)	Condenser RH (%)	S_R	Ambient conc. (#/cm^3)	Minor flow conc. (#/cm^3)	CEF
Dichotomous sampler	1.3*	10	60	27	30	46	14	95	1.2	23000	26000	1.1
	1.3*	10	60	35	35	98	16	95	3.0	23000	89000	3.9
	1.3*	10	60	25	34	99	12	95	3.8	12000	78000	6.5
	1.7*	10	35	27	34	98	15	95	3.1	30000	107000	3.6
	2.5	10	16.7	27	34	95	15	95	3.0	30000	65900	2.2
HVVI	1.0	10	150	28	28	74	15	95	1.7	8600	9240	1.1
	1.0	10	150	28	30	100	13	95	2.8	8800	39700	4.5
	1.0	10	150	28	32	98	12	95	3.3	8200	47700	5.8
	0.6*	10	350	23	22	21	7	95	0.6	24000	25000	1.0
	0.6*	10	350	25	27	100	11	95	2.7	17000	86000	5.1
HCPC	1.2	10	2000	27	28	98	11	95	2.9	13200	75200	5.7
	1.2	10	2000	27	29	98	9	95	3.4	7700	54000	7.0

*d_{50} values at flows other than designed values were theoretically calculated (assuming $\sqrt{\mathrm{St}} = 0.5$).
$^a r$ is the minor to total flow ratio of the virtual impactor, S_R is the supersaturatio ratio, CEF is the concentration enrichment factor defined as the ratio of the minor to ambient number concentration.

supersaturation ratio, as predicted by the theoretical model. More specifically, for supersaturation ratios above 1, particle penetration decreased with the supersaturation ratio. Furthermore, when the supersaturation ratio was <1, almost all of the incoming particles (minus the interstage losses in the impactor and the losses in the system itself) penetrated through the impactor, regardless of the impactor cutpoint. This indicates that the incoming ultrafine particles did not grow to supermicron sizes for supersaturation ratios <1. The results from Table 2 also imply that ultrafine particles did not grow to sizes bigger than 6.2 μm for a supersaturation ratio of 3. The 11% of the particles that apparently did not penetrate the 6.2 μm cutpoint impactor were assumed to have been lost in the apparatus (these losses were typically about 10%).

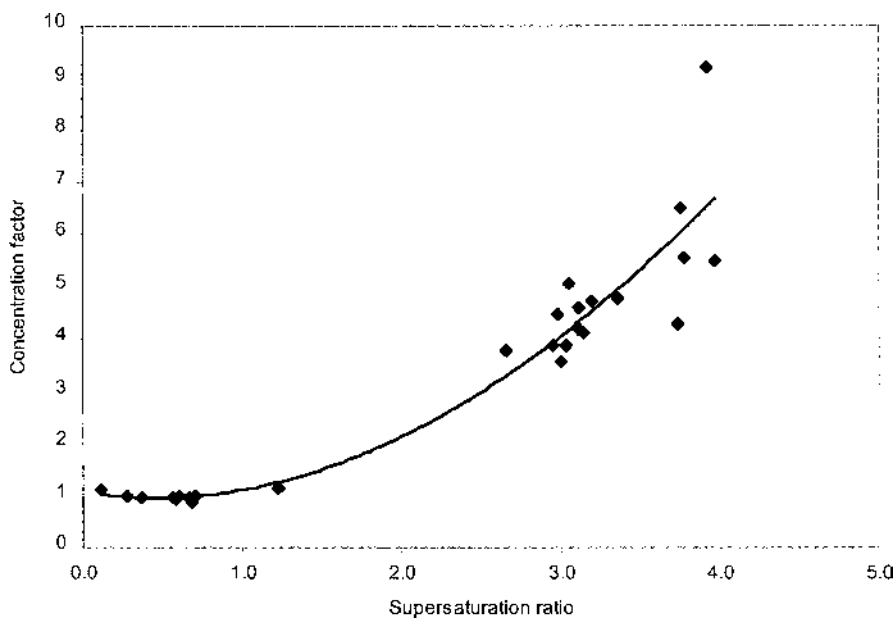

Figure 6. Concentration Factor (CF) as a function of supersaturation ratio (tests were conducted using a dichotomous sampler at $d_{50} = 1.3$ μm).

The particle penetrations for the 3.1 and 1.0 μm MOI stages were 28 and 9%, respectively, for a S_R ratio of about 3. This indicates that not all of the particles grew to sizes larger than 3.1 μm, but almost all grew to supermicron sizes. The 9% of particles found to penetrate the 1.0 μm cutpoint impactor may have been due to bounce-off of particles larger than 1.0 μm from the impactor substrate (Marple et al. 1991; Marple et al. 1993). In contrast, there was no insignificant difference between the particle penetration for the 1.0 and 1.8 μm stages. This indicates that a large majority of the particles grew to sizes above the 1.8 μm size. This is also supported by the theoretical calculations described above, which predict ultrafine particle growth to sizes between 2 and 3 μm for a supersaturation ratio of about 3. Similar results were reported for the prototype low volume condensational growth system investigated by Sioutas and Koutrakis (1996).

Virtual Impactor Experiments

Table 3 summarizes the results from the experiments of the virtual impactor experiments. As with the MOI experiments, the findings suggest that the supersaturation ratio is an important determinant of particle growth. No condensational growth to supermicron sizes occurred for ratios <1. Figure 6 shows the CEF for the dichotomous sampler as a function of the supersaturation ratio. Similar results were obtained for the other 2 virtual impactors.

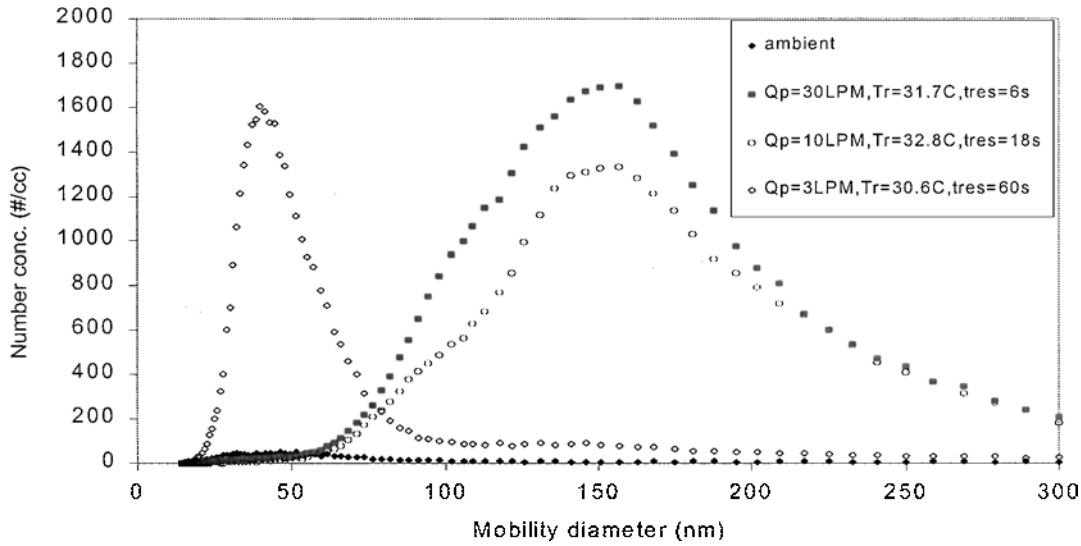

(a)

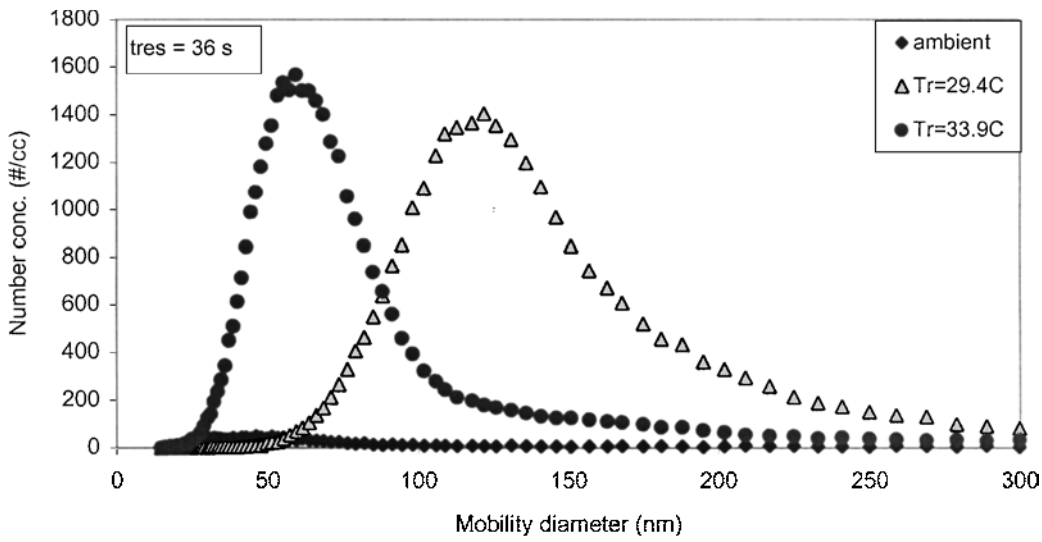

(b)

Figure 7. Thermal drying of condensationally grown particles as a function of residence time (aerosol flow) and reheat temperature: (a) Number particle concentration as a function of residence time; (b) Number particle concentration as a function of dryer temperature.

To minimize particle losses during the concentration/inertial separation process, it is important that particles grow to sizes significantly larger than the cutpoint of the virtual impactor (Marple et al. 1980). Therefore it is necessary to use a high enough supersaturation ratio to grow the ultrafine particles to sizes well above the cutpoint of the virtual impactor. In addition, the virtual impactor should be designed so that grown particles penetrate with minimum losses into the minor flow while avoiding excessive pressure drop in the minor flow, as required for animal inhalation studies. Based on these considerations, the ideal virtual impactor for the inertial separation of the grown particles should have a cutpoint near 1.0 μm. The main objective of these tests was to evaluate the performance of the developed condensational growth system, rather than optimizing the inertial separation/concentration system. However, our results suggest that the high volume condensational growth apparatus can be successfully combined with a virtual impactor to substantially increase the concentration levels of ambient air ultrafine particles.

Thermal Drying of Grown Particles

Three parameters were found to affect the rate of evaporational restoring of the grown particles: (a) the dryer temperature; (b) the residence time in the dryer; and (c) the particle number concentration of the aerosol entering the dryer.

Effect of Residence Time and Dryer Temperature. The results shown in Figures 7 a,b indicate that, as expected, both the dryer temperature and residence time (based on variation of aerosol flow) have a significant impact on the drying process. However, in order to minimize the semivolatile component losses, the dryer temperature should be close to atmospheric conditions as possible. Consequently, optimum conditions require keeping the temperature close to normal atmospheric values and using the minimum residence time sufficient for complete restoration of the ambient size distribution.

For example, for our thermal restoring system, at a 15 LPM aerosol flow, a temperature of about 30°C and a residence time of 60 s were adequate conditions to bring the grown particles back to their ambient size distribution. The evaporation time we experienced on our tube-type thermal dryer is larger than that predicted by the classical theoretical evaporation model described by Hinds (1999), which is based on certain homogenous temperature and relative humidity conditions. This is due to the fact that inside the tubes the conditions are not homogenous and depend on the complex heat and mass transfer phenomena.

Figure 8 illustrates that the ambient aerosol and the concentrated aerosol at the exit of the dryer have almost identical mean, median, and modal aerodynamic diameter. The concentration enrichment factor for this experiment was almost 17. This clearly indicates that the high volume condensational growth system can be combined successfully with a virtual impactor and a thermal dryer to grow, concentrate, and dry ultrafine particles, while maintaining the physico-chemical characteristics of the ambient particles.

Effect of Particle Number Concentration. Table 4 compares the size distribution of the particles at the entrance and exit of the dryer for 2 different particle number concentrations, while the residence time and temperature in the dryer were kept constant, 20 s and 30°C, respectively. For the low particle number concentration experiment, the thermal dryer brought particles back to almost their original size distribution. For the high particle number concentration experiment, particle size distribution was not restored to its original shape. This suggests that as the

Parameters	Ambient aerosol	Concentrated aerosol	Concentration enrichment factor
Mean mobility diameter (nm)	49.9	52.1	
Median mobility diameter (nm)	38.8	43.5	
Modal mobility diameter (nm)	38.5	40.0	
Total concentration (#/cm^3)	1972	33172	16.8

(a)

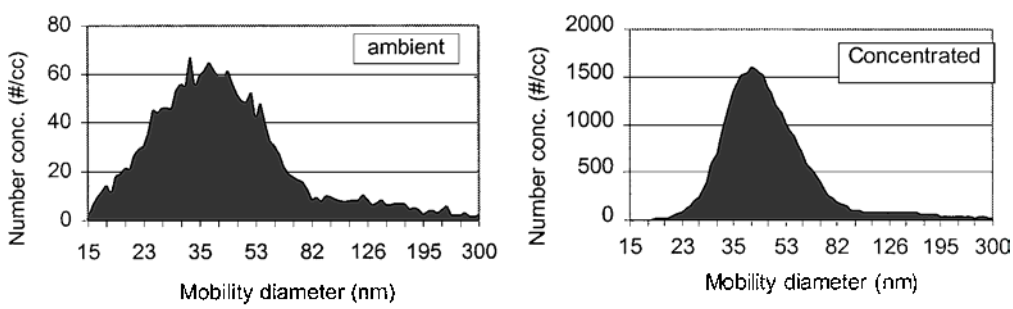

(b) (c)

Figure 8. Performance of developed thermal dryer (HCPC, $S_R = 3.2$, $T_r = 30.6°C$, $Q_{dryer} = 15$ LPM, tres = 60 s).

Table 4
Effect of water content of particles on the restoring process for ultrafine particles ($T_r = 30°C$)

Aerosol	Particle number concentration (#/cc)	Mean mobility diameter (nm)	Median mobility diameter (nm)	Modal mobility diameter (nm)	Particle water content[a] (g H_2O/Kg of air)
Sampled	8279	77.4	52.0	33.4	
Restored	35927	77.7	49.2	27.9	0.13
Sampled	2370	51.3	41.6	37.2	
Restored	94360	60.1	53.3	49.6	0.35

[a]Particle water content is calculated assuming that all particles grew to an average size of 2 μm.

particle number concentration increases, to obtain the complete size restoration it is necessary to use either a higher residence time or a higher dryer temperature. However, increasing the temperature may increase particle volatilization losses. Therefore if it is necessary, residence time can be increased in order to obtain the original ambient particle size distribution.

This can be explained by the difference in particle water content, which is assumed to be proportional to particle number concentration (Table 4; 0.13 versus 0.35 g/kg of air). This additional thermal mass due to the higher number concentration slows down the heating of particles and decreases the evaporation rate.

CONCLUSIONS

A high volume (2500 LPM) condensational growth system was developed. The system was evaluated using indoor air as a test aerosol. A series of inertial impactors were used to assess particle growth. This new high volume apparatus was shown to grow ambient ultrafine particles to supermicron sizes with minimum losses (about 10%). This system presents several features: it is fully automated and has computerized feedback controls. In addition, saturation of the aerosol with water vapor occurs at close to ambient temperatures to minimize particle losses of volatile components. Supersaturation ratios can be adjusted with optimum operational level in the range of 2 to 3 to ensure particle size increase to approximately 1.8 μm.

In an effort to overcome the limitations of previously used diffusion dryers as a means to dry condensationally grown particles, a thermal dryer-reshaper was used to restore particle size distribution. It was shown that thermal dryer performance depends on particle concentration, aerosol temperature, and residence time (aerosol flow).

Based on these prototype performance evaluation tests, we are in the process of constructing a new system that will operate at higher flow rates (5000 LPM) to grow, inertially separate and concentrate, and thermally restore ultrafine particles back to their original sizes. This new system will make it possible to perform extensive inhalation toxicological tests, including animal chamber exposures to concentrated ambient air ultrafine particles. These tests will be of paramount importance in efforts to investigate the health impacts of ambient ultrafine particles.

REFERENCES

Agarwal, J. K., and Sem, G. J. (1980). Continuous Flow, Single Particle Counting Condensation Nucleus Counter, *J. Aerosol Sci.* 11:343.

Ahn, K. H., and Liu, B. Y. H. (1990). Particle Activation and Droplet Growth Processes in Condensation Nucleus Counter—1: Theoretical Background, *J. Aerosol Sci.* 21:249–261.

Aitken, J. (1888). On the Number of Dust Particles in the Atmosphere, *Proc. R. Soc. Edinb.* 16:135.

Bricard, J., Delattre, P., Madelaine, G., and Pouprix, M. (1976). *In Fine Particles*, edited by B. Y. H. Liu, Academic Press, New York.

Clark, R. W., Coull, B., Reinisch, U., Catalano, P., Killingsworth, C., Koutrakis, P., Kavouras, I., Murthy, G. G., Krishna, I., Lawrence, J., Lovett, E., Wolfson, M., Verrier, R., and Godleski, J. (2000). Inhaled Concentrated Ambient Particles Induce Pulmonary Inflammation and Hematological Changes in Canines, *Environmental Health Perspectives* 108:1179–1187.

De la Mora, F., Hering, S. V., Rao, N., and McMurry, P. (1990). Hypersonic Impaction of Ultrafine Particles, *J. Aerosol Sci.* 21:169–187.

Demokritou, P., Gupta, T., and Koutrakis, P. (2002). Development and Laboratory Characterization of a Prototype Coarse Particle Concentrator for Inhalation Toxicological Studies, *J. Aerosol Sci.* 33:1111–1123.

Demokritou, P., Kavouras, I. G., Ferguson, S. T., and Koutrakis, P. (2002). Development of a High Volume Cascade Impactor for Toxicological and Chemical Characterization Studies, *Aerosol Sci. Technol.* 36:925–933.

Ding, Y., and Koutrakis, P. (2000). Development of a Dichotomous Slit Nozzle Virtual Impactor, *J. Aerosol Sci.* 31:1421–1431.

Dockery, D. W., and Pope, C. A. (1994). Acute Effects of Particulate Air Pollution, *Ann. Rev. Pub. Health* 15:107–132.

Dockery, D. W., Pope, C. A., Xu, X., Spengler, J. D., Ware, J. H., Fay, M. E., Ferris, B. G., and Speizer, F. E. (1993). An Association Between Air Pollution and Mortality in Six U.S. Cities, *New Eng. J. Medicine* 329:1753–1808.

Drinker, P., Thomson, R. M., and Finn, J. L. (1927). Metal Fume Fever II: Resistance Acquired by Inhalation of Zinc Oxide on Two Successive Days, *J. Ind. Hyg. Toxicol.* 9:98–105.

Ferron, G., and Soderholm, S. (1990). Estimation of the Time for Evaporation of Pure Water Droplets and for Stabilization of Salt Solution Particles, *J. Aerosol Sci.* 21:415–429.

Fuchs, N. A., and Sutugin, A. G. (1970). *Highly Dispersed Aerosols*, Chap. 3, Ann Arbor Science Publishers, Ann Arbor, MI.

Gamble, J. (1998). $PM_{2.5}$ and Mortality in Long Term Prospective Cohort Studies: Cause Effects or Statistical Associations, *Environ. Health Perspect.* 106(9):535–549.

Godleski, J., Sioutas, C., Katler, M., and Koutrakis, P. (1996). Death from Inhalation of Concentrated Ambient Air Particles in Animal Models of Pulmonary Disease, *Resp. and Crit. Care Med.* 155(4):A246.

Gordon, T., Chen, L. C., Fine, J. M., Schleisinger, R. B., Su, W. Y., Kimmel, T. A., and Amdur, M. O. (1992). Pulmonary Effects of Zinc Oxide in Human Subjects, Guinea Pigs, Rats, and Rabbits, *Am. Ind. Hyg. Assoc. J.* 53:503–509.

Hering, S. V., and Stolzenburg, M. R. (1995). On-Line Determination of Particle Size and Density in the Nanometer Size Range, *Aerosol Sci. Technol.* 23:155–173.

Hinds, W. (1999). *Aerosol Technology*, John Wiley & Sons Inc., New York.

ICRP, International Commission on Radiological Protection (1994). *Human Respiratory Tract Model for Radiological Protection: A Report of Committee 2 of the ICRP*, Pergamon Press, Oxford.

Kavouras, I., Mihalopoulos, N., and Stephanou, E. (1998). Formulation of Atmospheric Particles from Organic Acids Produced by Forests, *Nature* 395:683–686.

Kidwell, C. B., and Ondov, J. M. (2001). Development and Evaluation of a Prototype System for Collecting Sub-Hourly Ambient Aerosol for Chemical Analysis, *Aerosol Sci. Technol.* 35:596–601.

Kim, S., Chang, M. C., Kim, D., and Sioutas, C. (2000). A New Generation of Portable Coarse, Fine and Ultrafine Particle Concentrators for Use in Inhalation Toxicology, *Inhal. Toxicol.* 12(supplement):121–137.

Kotzick, R., and Niessner, R. (1999). The Effects of Aging Processes on Critical Supersaturation Ratios of Ultrafine Carbon Aerosols, *Atmos. Environ.* 33:2669–2677.

Kotzick, R., Panne, U., and Niessner, R. (1997). Changes in Condensation Properties of Ultrafine Carbon Particles Subjected to Oxidation by Ozone, *J. Aerosol Sci.* 28:725–735.

Marple, V. A., and Chien, M. C. (1980). Virtual Impactors: A Theoretical Study, *Environ. Sci. Technol.* 45:673–874.

Marple, V. A., Rubow, K. L., and Behm, S. M. (1991). A Microorifice Uniform Deposit Impactor (MOUDI): Description, Calibration, and Use, *Aerosol Sci. Technol.* 14:434–446.

Marple, V. A., Rubow, K. L., and Olson, B. A. (1993). Inertial, Gravitational, Centrifugal and Thermal Collection Techniques. In *Aerosol Measurement*, edited by K. Willeke and P. A. Baron, Van Nostrand Reinhold, New York, pp. 106–232.

Oberdorster, G., Ferin, J., and Lehnert, B. E. (1994). Correlation Between Particle Size, in vivo Particle Persistence and Lung Injury, *Environ. Health Perspect.* 102:173–179.

Olawoyin, O. O., Raunemaa, T. M., and Hopke, P. K. (1995). A System for Aerodynamically Sizing Ultrafine Radioactive Particles, *Aerosol Sci. Technol.* 23:121–130.

Peters, A., Verrier, R. L., Schawrtz, J., Gold, D. R., Mittleman, M., Baliff, J., Oh, J. A., Allen, G., Monahan, K., and Dockery, D.W. (2000). Air Pollution and Incidence of Cardiac Arrythmia, *Epidemiol.* 11:11–17.

Pope, C. A., Verrier, R. L., Lovett, E. G., Larson, A. C., Raizenne, M. E., Kanner, R. E., Schwartz, J., Villegas, M., Gold, D. R., and Dockery, D. W. (1999). Heart Rate Variability Associated with Particulate Air Pollution, *Amer. Heart. J.* 138:890–899.

Schwartz, J., and Dockery, D. W. (1992). Increased Mortality in Philadelphia Associated with Daily Air Pollution Concentrations, *Am. J. Epidemiol.* 135:12–19.

Seinfeld, J. H. (1991). *Atmospheric Chemistry and Physics of Air Pollution*, Wiley, New York.

Sinclair, D., and Hoops, G. S. (1975). A Continuous Flow Condensation Nucleus Counter, *J. Aerosol Sci.* 6:1.

Sioutas, C., Kim, S., and Chang, M. (1999). Development and Evaluation of a Prototype Ultrafine Particle Concentrator, *J. Aerosol Sci.* 30:1001–1017.

Sioutas, C., and Koutrakis, P. (1996). Inertial Separation of Ultrafine Particles using a Condensational Growth/Virtual Impaction system, *Aerosol Sci. Technol.* 25:424–436.

Sioutas, C., Koutrakis, P., and Burton, R. (1995). A Technique to Expose Animals to Concentrated Fine Ambient Aerosols, *Env. Health Perspectives*, 103:172–177.

Whitby, K. T., and Svendrup, G. M. (1980). California Aerosols: Their Physical and Chemical Characteristics, *Environ. Sci. Technol.* 10:477.

Zhang, Z. Q., and Liu, B. Y. H. (1990). Dependence of the Performance of TSI 3020 Condensation Nucleus Counter on Pressure, Flow Rate, and Temperature, *Aerosol Sci. Technol.* 13:493–504.